ROZPRAWY INŻYNIERSKIE • ENGINEERING TRANSACTIONS • 35, 4, 591-609, 1987
Polska Akademia Nauk • Instytut Podstawowych Problemów Techniki

MODE INTERACTION IN WIDE PLATE WITH CLOSED SECTION LONGITUDINAL STIFFENERS UNDER COMPRESSION

Z. KOŁAKOWSKI (ŁÓDŹ)

Interaction of nearly simultaneous buckling modes in the presence of imperfections is studied. The investigation is concerned with an infinitely wide plate having thin-walled longitudinal stiffeners of trapezoid cross-section under uniform compression. In these structures a few modes are of particular interest, namely an overall long-wave buckling mode of the whole structures and local short-waves buckling modes, respectively. The asymptotic expansion established by BYSKOV and HUTCHINSON [1] is also used here. The present paper is devoted to the study of equilibrium paths in the advanced post-buckling region of an imperfect stiffened plate. The bifurcation stress is determined analytically and the asymptotically exact expansion is obtained for the initial post-bifurcation behaviour. The calculations are carried out for several types of plates with closed section longitudinal stiffeners.

1. NOTATION

E Young's modulus,
ν Poisson's ratio,
D_i flexural rigidity,
l length of the stiffened plate,
b_i width of wall i of the plate,
h_i thickness of wall i of the plate,
x_i, y_i, z_i local coordinate system for wall i of the plate,
u_i, v_i, w_i displacements of the middle surface,
$\overset{0}{u}_f, \overset{0}{v}_i, \overset{0}{w}_i$ prebuckling displacement fields,
$\overset{n}{u}_i, \overset{n}{v}_i, \overset{n}{w}_i$ buckling displacement fields,
N_{ix}, N_{iy}, N_{ixy} in-plane stress resultants for wall i,
M_{ix}, M_{iy}, M_{ixy} bending moment resultants for wall i,
Q_i Eq. (3.6),
λ scalar load parameter,
n number of mode,
λ_1 value of λ at overall mode bifurcation,
λ_2, λ_3 values of λ at local mode bifurcation,
λ_s maximum value of λ for imperfect stiffened plate,
ξ_1 amplitude of overall buckling mode,
ξ_2, ξ_3 amplitudes of local buckling modes,

$\bar{\xi}_n$ imperfection amplitude corresponding to ξ_n
Δ measure of the applied pressure,
m number of axial half-waves of mode number n,
a_{ijj} postbuckling coefficients (see Appendix),
$d_2\, d_3$ postbuckling coefficients (Eq. (4.5)),
$z_1 = -d_3\, \xi_1$,
$z_2 = \sqrt{2d_2\, d_3}\, \xi_2$ generalized displacement parameters,
$\bar{z}_1, \bar{z}_2$ generalized imperfection parameters (Eq. (4.7)),
$\sigma_1^*, \sigma_2^*, \sigma_3^*$ dimensionless global and local stresses
$\sigma_{\min}^* = \min(\sigma_1^*, \sigma_2^*)$,
σ_s^* limit dimensionless stress,
A cross sectional area of the stiffener,
I moment of intertia of the stiffener by the central line of the thin-walled plate (skin plate),
σ_E^* dimensionless stress obtained in [19].

$$s = l \Big/ \left\{ \left[\frac{h_1^3}{12(1-\nu^2)} + \frac{I}{(b_1+b_4)} \right] \Big/ \left[\frac{h_1}{(1-\nu^2)} + \frac{A}{(b_1+b_4)} \right] \right\}^{\frac{1}{2}}$$ — equivalent slenderness ratio.

2. Introduction.

In compression members containing thin plates, local buckling of the plate elements and Euler type buckling of the whole structure can occur. Interaction between the independent buckling modes may result in an imperfection-sensitive structure. In recent years more and more papers are being devoted to the analysis of the interaction of buckling modes as a factor that determines the construction sensitivity to imperfections at nearly the same magnitudes of bifurcational loads corresponding to different modes and to the closely related problem of optimum structural design.

The simplest possible model of a column (given from [21]), depicted in Fig. 1a, consists of a rigid bar supported on an elastic hinge. This simple model is employed in several elementary text-books. The perfect column, with zero eccentricity of the applied load ($e = \varkappa, L = 0$), loses its stability and buckles by bifurcation at the critical load $P_1 = D/L$. The post-buckling behaviour depends on nonlinearities in the spring characteristic. The three commonly occurring types of buckling behaviour are shown in Fig. 1b, namely asymmetric, unstable-symmetric and stable-symmetric. Equilibrium paths in the close neighbourhood of the bifurcation point have a very distinct form in each case. A small imperfection in such systems causes a comparatively large change in the critical load. In cases of an unstable descending post-buckling path ($\alpha \neq 0$ or $\alpha = 0, \beta < -1/6$) the column is sensitive to geometric imperfections or load eccentricity. In the absence of a descending post-buckling path of the perfect column no loss of stability

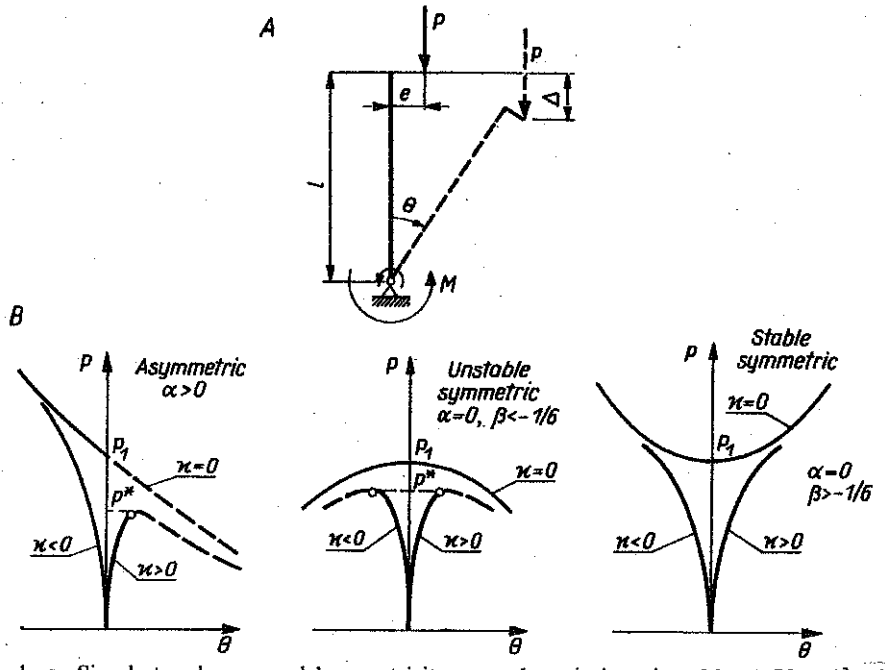

FIG. 1. a. Simplest column model eccentricity $e = \varkappa L$, spiral spring $M = D\,[\theta - \alpha\theta^2 + \beta\theta^3]$, b. Load-deflection curves.

occurs in the column with imperfections or a load eccentricity. The presence of the buckling load P_1 of the perfect column appears here only in the form of a marked increase of the deflection when the load P approaches and passes the value P_1. These results show that the critical load in such structures may be extremely sensitive to small variations in imperfections, particularly when these are near zero.

The constructions shaped as an infinitely wide plate and as a closed cylindrical shell, strengthened by longitudinal stiffeners have been analysed in a most detailed manner with application of general methods of stability analysis of constructions, susceptible to imperfections [1, 2, 3 and 4]. TVERGAARD [5] has studied a post-bifurcational equilibrium path of a compressed wide plate with longitudinal stiffeners of rectangular section. He has modelled the eccentric stiffeners by beams which, at buckling, turn together with the plate by the same angle, and in [6] he has analysed the optimum design of the plates ribbed in this manner. KOITER and PIGNATARO [3], by means of an approximate energetic approach, observed a high sensitivity of stiffened plates at small imperfections for simultaneous modes of local and global buckling.

The authors assumed a simplified expression for skin plate displacements and neglected the effect of normal stress σ_y and shear strain γ_{xy}. VAN DER NEUT [7] has performed an analysis of cooperation of buckling modes

of a plate strengthened with tophat stringers. He considered a simplified model consisting of two load carrying flanges connected by webs rigid in shear and laterally. The influence of local ad global mode of buckling has also been considered.

A general theory of interaction of buckling modes of stiffened plates was developed by Koiter [4], by means of a generalization of the approach, presented in [3]. This theory is an approximation of strain energy by one-dimensional amplitude functions, corresponding to the established deformation modes in the longitudinal direction. Those approximations enable a relatively simple consideration of stationarity of the energy functional in the theory of continuous media. Such an approach made it possible to investigate several configurations of plates strengthened with various stiffeners.

Another general approach may be developed using the method of extension of bifurcational analysis in the post-buckling region [8]. This approach is advantageous because it applies Kármán's more general nonlinear theory. In papers [9] and [10] stiffened plates are considered as plates, connected elastically along the contact line, simply-supported on loaded edges and free at the fourth edge. The post-buckling state of plates is described by Karmán's nonlinear equation.

On the ground of results of the general, asymptotic stability theory, a solution of the nonlinear problems of stability of the stiffened plate with regard to the buckling mode interaction has been achieved by MANEVIČ [11]. Differences have been shown between the situations, when the beam- and plate-model of stiffener has been assumed. Following the energetic method, SEDLACEK [12] accomplished an analysis of a local loss of stability of a compressed plate, strengthened with open and closed stringers.

Paper [13] has been devoted to an analysis of orthotropic stability of a plate with a longitudinal stiffener, subject to compression. The plate stability was determined by applying a transition matrix, the beam- (beam subjected to bending and torsion) and plate- (stiffener modelling by a plate, elastically connected with skin plate) model of stiffener being assumed.

MANEVIČ [14] has determined a post-bifurcational equilibrium path of a wide plate, and in [15] of a cylindrical shell strengthened with longitudinal stiffeners of the rectangular section, whereas in [16] he has analysed the buckling of a plate and cylindrical shell strengthened with stiffeners of T-bar section. In all these papers a plate-model of stiffeners was assumed. In [1, 2, 17] the sensitivity of cylindrical stiffened shells to imperfections has been determined assuming the beam-model.

In the present paper the initial post-buckling behaviour of a wide plate with the thin-walled trapezoidal section longitudinal stiffeners being under compression is examined in the elastic range on the basis of Byskov and Hutchinson's method, taking account of the cooperation between all the walls of stiffened plate.

3. Structural problem

A simply-supported plate of infinite width with longitudinal regularly arranged closed stiffeners is considered in the present paper.

Basic geometrical dimensions of the investigated plate and assumed local coordinate systems are presented in Fig. 2. The materials of the column

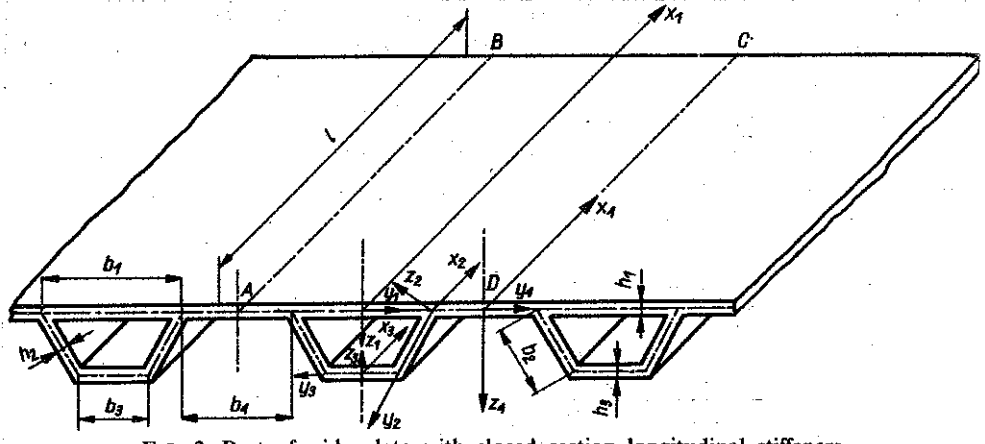

FIG. 2. Part of wide plate with closed section longitudinal stiffeners.

obey Hooke's law. When u_i, v_i, w_i are the displacements of the middle surface in the x_i, y_i and z_i directions, the membrane strains of the wall i are obtained as:

$$\begin{aligned} \varepsilon_{ix} &= u_{i,x} + 0{,}5\,(w_{i,w}^2 + v_{i,x}^2), \\ \varepsilon_{iy} &= v_{i,y} + 0{,}5\,(w_{i,y}^2 + u_{i,y}^2), \\ \gamma_{ixy} &= u_{i,y} + v_{i,x} + w_{i,x}\,w_{i,y} \end{aligned} \tag{3.1}$$

and the bending strains are given by

$$\varkappa_{ix} = -w_{i,xx}, \qquad \varkappa_{iy} = -w_{i,yy}, \qquad \varkappa_{ixy} = -w_{i,xy}. \tag{3.2}$$

The relationships among stresses and strains for the wall i have the following forms:

$$\begin{aligned} N_{ix} &= \frac{Eh_i}{1-\nu^2}\,(\varepsilon_{ix} + \nu\varepsilon_{iy}), & M_{ix} &= +D_i\,(\varkappa_{ix} + \nu\varkappa_{iy}), \\ N_{iy} &= \frac{Eh_i}{1-\nu^2}\,(\varepsilon_{iy} + \nu\varepsilon_{ix}), & M_{iy} &= +D_i\,(\varkappa_{iy} + \nu\varkappa_{ix}), \\ N_{ixy} &= \frac{Eh_i}{2\,(1+\nu)}\,\gamma_{ixy}, & M_{ixy} &= +D_i\,(1-\nu)\,\varkappa_{ixy}. \end{aligned} \tag{3.3}$$

The differential equilibrium equations resulting from the virtual work expression for one wall can be written as

$$
\begin{aligned}
&-N_{ix,x}-N_{ixy,y}=0,\\
&-(N_{ix}\,v_{i,x})_{,x}-N_{iy,y}-N_{ixy,x}=0,\\
&-(N_{ix}\,w_{i,x})_{,x}-(N_{iy}\,w_{i,y})_{,y}-N_{ixy,y}\,w_{i,x}-\\
&\qquad -2N_{ixy}\,w_{i,xy}-N_{ixy,x}\,w_{i,y}+D_i\,\nabla\nabla w_i=0.
\end{aligned}
\tag{3.4}
$$

In case of a sufficient number of stiffeners, the condition of geometrical regularity may be applied and the analysis may be restricted to one, arbitrarily selected segment *ABCD* (Fig. 2). Due to a very high torsional rigidity of closed stiffeners, a vertical symmetry axis has been assumed for the segment under consideration.

The geometrical and statical continuity conditions at the junctions of plates may be written as

$$
\begin{aligned}
&w_1\left(x,\,y=\frac{b_1}{2}\right)\equiv w_1|^{+}=w_2\,(x,\,y=0)\cos\alpha+v_2\,(x,\,y=0)\sin\alpha\equiv\\
&\qquad\equiv w_2|^{0}\cos\alpha+v_2|^{0}\sin\alpha=w_4\left(x,\,y=-\frac{b_4}{2}\right)\equiv w_4|^{-},\\
&v_1|^{+}=v_2|^{0}\cos\alpha-w_2|^{0}\sin\alpha=v_4|^{-},\\
&-w_3\left(x,\,y=-\frac{b_3}{2}\right)\equiv -w_3|^{-}=w_2\,(x,\,y=b_2)\cos\alpha+\\
&\qquad +v_2\,(x,\,y=b_2)\sin\alpha\equiv w_2|^{+}\cos\alpha+v_2|^{+}\sin\alpha,\\
&v_3|^{-}=w_2|^{+}\sin\alpha-v_2|^{+}\cos\alpha,\\
&w_{1,y}|^{+}=w_{2,y}|^{0}=w_{4,y}|^{-},\\
&w_{2,y}|^{+}=w_{3,y}|^{-},\\
&D_1\,(w_{1,yy}+\nu w_{1,xx})|^{+}-D_2\,(w_{2,yy}+\nu w_{2,xx})|^{0}-\\
&\qquad -D_4\,(w_{4,yy}+\nu w_{4,xx})|^{-}=0,\\
&D_2\,(w_{2,yy}+\nu w_{2,xx})|^{+}-D_3\,(w_{3,yy}+\nu w_{3,xx})|^{-}=0,\\
&\varepsilon_{1x}|^{+}=\varepsilon_{2x}|^{0}=\varepsilon_{4x}|^{-},\\
&\varepsilon_{2x}|^{+}=\varepsilon_{3x}|^{-},\\
&N_{1y}|^{+}-N_{2y}|^{0}\cos\alpha+Q_{2y}|^{0}\sin\alpha-N_{4y}|^{-}=0,\\
&N_{3y}|^{-}+N_{2y}|^{+}\cos\alpha-Q_{2y}|^{+}\sin\alpha=0,\\
&Q_{1y}|^{+}-N_{2y}|^{0}\sin\alpha\,Q_{2y}|^{0}\cos\alpha-Q_{4y}|^{-}=0,\\
&Q_{3y}|^{-}+N_{2y}|^{+}\sin\alpha+Q_{2y}|^{+}\cos\alpha=0,\\
&N_{1xy}|^{+}-N_{2xy}|^{0}-N_{4xy}|^{-}=0,\\
&N_{2xy}|^{+}-N_{3xy}|^{-}=0,
\end{aligned}
\tag{3.5}
$$

where

$$
\alpha=\arccos\left(\frac{b_3-b_1}{2b_2}\right),
$$

$$
Q_{iy}=N_{iy}\,w_{i,y}+N_{ixy}\,w_{i,x}-D_i\,[w_{i,yyy}+(2-\nu)\,w_{i,xxy}].
\tag{3.6}
$$

4. Method of solution

The stiffened plate is loaded by the uniform axial compression. The prebuckling solution consists of homogeneous fields and we may take

$$\begin{aligned} \overset{0}{u}_i &= -x_1 \Delta, \\ \overset{0}{v}_i &= v y_i \Delta, \\ \overset{0}{w}_i &= 0, \end{aligned} \qquad i = 1, 2, 3, 4. \tag{4.1}$$

The boundary conditions permit the first order solution that determines the initial post-bifurcation behaviour to be written as

$$\begin{aligned} \overset{n}{w}_i &= (\overset{n}{C}_{1i} \operatorname{ch} \overset{n}{r}_{1i} y_i + \overset{n}{C}_{2i} \operatorname{sh} \overset{n}{r}_{1i} y_i + \overset{n}{C}_{3i} \cos \overset{n}{r}_{2i} y_i + \\ &\quad + \overset{n}{C}_{4i} \sin \overset{n}{r}_{2i} y_i) \sin \frac{m\pi x}{l}, \\ \overset{n}{u}_i &= (\overset{n}{C}_{5i} \operatorname{ch} \overset{n}{r}_3 y_i + \overset{n}{C}_{6i} \operatorname{sh} \overset{n}{r}_3 y_i + \overset{n}{C}_{7i} \operatorname{ch} \overset{n}{r}_4 y_i + \\ &\quad + \overset{n}{C}_{8i} \operatorname{sh} \overset{n}{r}_4 y_i) \cos \frac{m\pi x}{l}, \\ \overset{n}{v}_i &= (-\overset{n}{C}_{5i} \overset{n}{b}_1 \operatorname{sh} \overset{n}{r}_3 y_i - \overset{n}{C}_{6i} \overset{n}{b}_1 \operatorname{ch} \overset{n}{r}_3 y_i - \overset{n}{C}_{7i} \overset{n}{b}_2 \operatorname{sh} \overset{n}{r}_4 y_i - \\ &\quad - \overset{n}{C}_{8i} \overset{n}{b}_2 \operatorname{ch} \overset{n}{r}_4 y_i) \sin \frac{m\pi x}{l}, \end{aligned} \tag{4.2}$$

where

$$\begin{aligned} \overset{n}{r}_{1i} &= \sqrt{\frac{m\pi}{l}\left[\frac{m\pi}{l} + \sqrt{\frac{12(1-\nu^2)\lambda\Delta}{h_i^2}}\right]}, \\ \overset{n}{r}_{2i} &= \sqrt{-\frac{m\pi}{l}\left[\frac{m\pi}{l} - \sqrt{\frac{12(1-\nu^2)\lambda\Delta}{h_i^2}}\right]}, \\ \overset{n}{e}_1 &= \frac{1-\nu}{2}, \\ \overset{n}{e}_2 &= (1-\nu)\left(\frac{m\pi}{l}\right)^2 \left(\frac{1-\nu^2}{2}\lambda\Delta - 1\right), \\ \overset{n}{e}_3 &= (1-\nu^2)^2 \left(\frac{m\pi}{l}\right)^4 \left[\frac{1}{4}\lambda^2\Delta^2(1-\nu^2) + \lambda\Delta\right], \\ \overset{n}{r}_3 &= \sqrt{\frac{-\overset{n}{e}_2 + \sqrt{\overset{n}{e}_3}}{2\overset{n}{e}_1}}, \\ \overset{n}{r}_4 &= \sqrt{\frac{-\overset{n}{e}_2 - \sqrt{\overset{n}{e}_3}}{2\overset{n}{e}_1}}, \end{aligned} \tag{4.3}$$

(4.3) [cont.]
$$\overset{n}{b}_1 = \frac{1-\nu}{1+\nu}\,\frac{\overset{n}{r}_3}{\frac{m\pi}{l}} - \frac{2\frac{m\pi}{l}}{\overset{n}{r}_3(1+\nu)},$$

$$\overset{n}{b}_2 = \frac{1-\nu}{1+\nu}\,\frac{\overset{n}{r}_4}{\frac{m\pi}{l}} - \frac{2\frac{m\pi}{l}}{\overset{n}{r}_4(1+\nu)}.$$

Since the perpendicular axis of symmetry of the cross-section is assumed, the coefficients $\overset{n}{C}_{2i}, \overset{n}{C}_{4i}, \overset{n}{C}_{6i}, \overset{n}{C}_{8i}$ at $i = 1, 3$ in Eqs. (4.2) vanish. For some values of load parameter the trigonometric functions $(4.2)_1$ have to be transformed into suitable hyperbolic functions. The bifurcation buckling load λ_n is the smallest value of the parameter for any integral value of m for which the determinant of the conditions (3.5) vanishes. The overall buckling mode, occurring at $m = 1$, is denoted by $\overset{1}{w}_i, \overset{1}{u}_i, \overset{1}{v}_i$ and the local buckling mode, occurring at $m \neq 1$, is denoted by $\overset{n}{w}_i, \overset{n}{u}_i, \overset{n}{v}_i$ where $n > 1$.

All the buckling modes are normalized so that the maximum normal displacement of the first wall is equal to the plate thickness h_1. In the case when the value of λ_2 and λ_3 are close for two local buckling modes at different numbers of half-waves m, a set of three nonlinear equations has been solved. However, in this instance the interaction of both local modes is very weak or does not even occur. Therefore the interaction of the global mode and each of the local modes may be considered separately. According to the assumptions made in BYSKOV and HUTCHINSON'S theory [1], local buckling modes do not interact explicitely. However, the interaction occurs through the interaction of each of them with the global mode. The formulas for the post-buckling coefficients a_{ijJ} (see Appendix) involve only buckling modes. After neglecting the values vanishingly small, the equilibrium path is governed by

(4.4)
$$\left(1-\frac{\lambda}{\lambda_1}\right)\xi_1 + \xi_2^2\, d_2 = \frac{\lambda}{\lambda_1}\,\bar{\xi}_1,$$
$$\left(1-\frac{\lambda}{\lambda_2}\right)\xi_2 + \xi_1\,\xi_2\, d_3 = \frac{\lambda}{\lambda_2}\,\bar{\xi}_2,$$

where $d_2 = a_{221}$,

(4.5)
$$d_3 = a_{122} + a_{212}.$$

In the points where the scalar load parameter λ_s reaches the maximum value for the imperfect structure (bifurcation or limit points), the Jacobian of the system (4.4) is equal to zero

$$(4.6)\qquad \left(\frac{\lambda_s}{\lambda_2}\right)^2 \frac{\lambda_2}{\lambda_1}+\frac{\lambda_s}{\lambda_2}\left(1+\frac{\lambda_2}{\lambda_1}+\bar{z}_1\frac{\lambda_2}{\lambda_1}\right)+1-\frac{3}{2}\left[\left(1-\frac{\lambda_s}{\lambda_1}\right)\frac{\lambda_s}{\lambda_2}\bar{z}_2\right]^{2/3}=0,$$

where

$$(4.7)\qquad \bar{z}_1=-\bar{\xi}_1 d_3,\qquad \bar{z}_2=\sqrt{2d_2 d_3}\,\bar{\xi}_2.$$

The expression (4.6) is an implicit equation of surface $\lambda_s=f(\bar{\xi}_1,\bar{\xi}_2)$ (surface of imperfection sensitivity). The parameters $\bar{z}_1$, $\bar{z}_2$ may be called generalized-imperfection parameters.

Equation (4.6) takes the same form as in [11] where a more detailed analysis of the discussed equation has been given.

5. Results of numerical calculations

The detailed numerical calculations for several different wide plates with thin-walled trapezoidal section longitudinal stiffeners the geometry of which

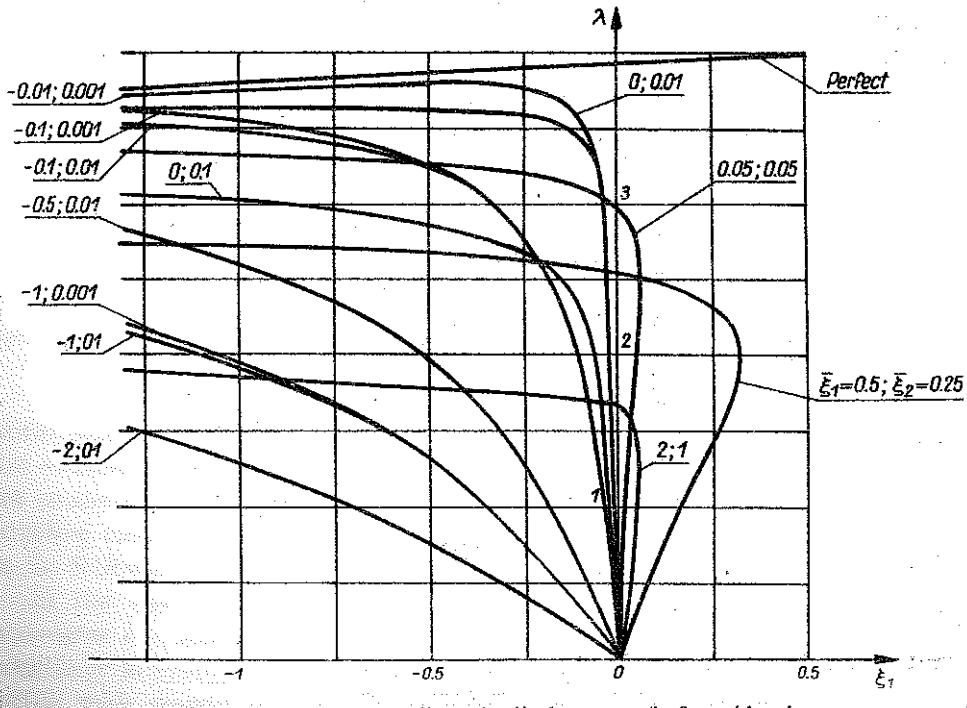

FIG. 3. Load versus overall mode displacement ξ_1 for wide plate $b_2/b_1=0.7166$, $b_3/b_1=0.4933$, $b_4/b_1=1.0$, $l/b_1=12$, $h_2/h_1=0.6$, $h_3/h_1=0.6$, $b_1/h_1=30$, $m=13$.

Table 1. Results of calculations for several types of stiffened plates with trapezoidal section stiffeners

b_2/b_1	b_3/b_1	b_4/b_1	l/b_1	h_2/h_1	h_3/h_1	b_1/h_1	σ_1^*	m	σ_2^*	d_2	d_3	σ_E^*
0.7166	0.4933	1.0	12.0	0.6	0.6	30.0	3.9449	13 20	3.9106 3.9349	1.56392 −87.612	0.03283 −0.07071	4.701
0.9866	0.3000	1.0	21.15	0.6	0.6	30.0	2.2254	29	2.2029	−738.96	−0.05623	2.572
0.9633	0.4500	1.0	21.927	0.6	0.6	30.0	2.2841	30	2.2707	−623.40	−0.04964	2.518
1.2233	0.3000	1.0	33.75	0.6	0.6	30.0	1.4588	38	1.4571	−1613.34	−0.04031	1.592
0.7166	0.4933	1.333	13.947	0.6	0.6	30.0	2.7637	12	2.7808	6.5263	0.06176	3.261
0.7166	0.4933	1.6666	16.48	0.6	0.6	30.0	1.8734	12	1.8884	15.5552	0.06196	2.192

is known from literature [12, 19 and 20] have been performed. The assumed geometrical parameters and obtained results of calculations are presented in Table 1.

The length of the stiffened plate l has been chosen so that local and global buckling occurs nearly simultaneously. The nondimensional stress $\sigma_n^* = \frac{\sigma_n}{E} 10^3 = \lambda_n \Delta 10^3$ at $n = 1, 2, 3$, $\nu = 0, 3$ instead of the local parameter λ_n, the number of half-waves m for local modes, coefficients d_2, d_3 of a non-

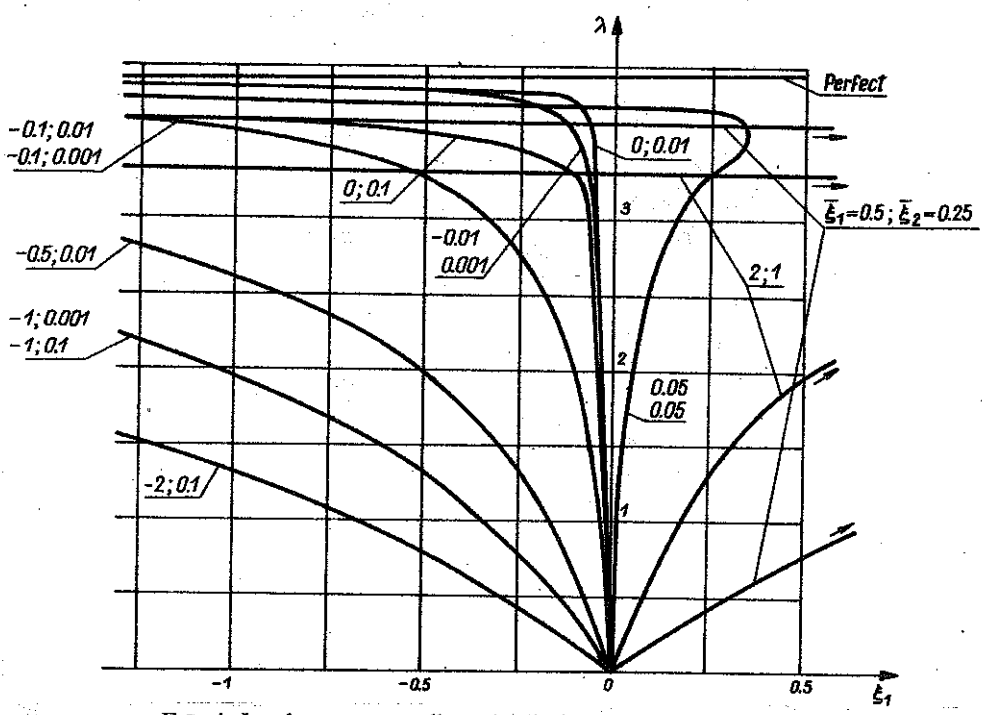

FIG. 4. Load versus overall mode displacement ξ_1 for wide plate $b_2/b_1 = 0.7166$, $b_3/b_1 = 0.4933$, $b_4/b_1 = 1.0$, $l/b_1 = 12$, $h_2/h_1 = 0.6$, $h_3/h_1 = 0.6$, $b_1/h_1 = 30$, $m = 15$.

linear system of equations (4.4) and dimensionless stress σ_E^{**} obtained from the technical theory in [19] are shown in Table 1. Initial imperfections are considered in the shape of the wide plate buckling mode and the local buckling mode, and their amplitudes are denoted by $\bar{\xi}_1$ and $\bar{\xi}_2$, respectively. In the following ξ_1 and ξ_2 denote the additional growth of these two modes.

In the next three figures the relationship between ξ_1 and the load parameter λ is shown. For the plates in Figs. 3, 4 and 5, the post-bifurcation behaviour is symmetric with respect to the mode amplitude ξ_2 and asymmetric with respect to the amplitude ξ_1 as predicted by the asymptotic analysis.

The local mode imperfections (positive or negative) promote an interaction between the local and the global mode. The local mode imperfections promote failure by causing a rapid growth of ξ_1. In Figs. 3 and 5 a load carrying capacity with imperfections ξ_1 and ξ_2 is marked by a crosslet.

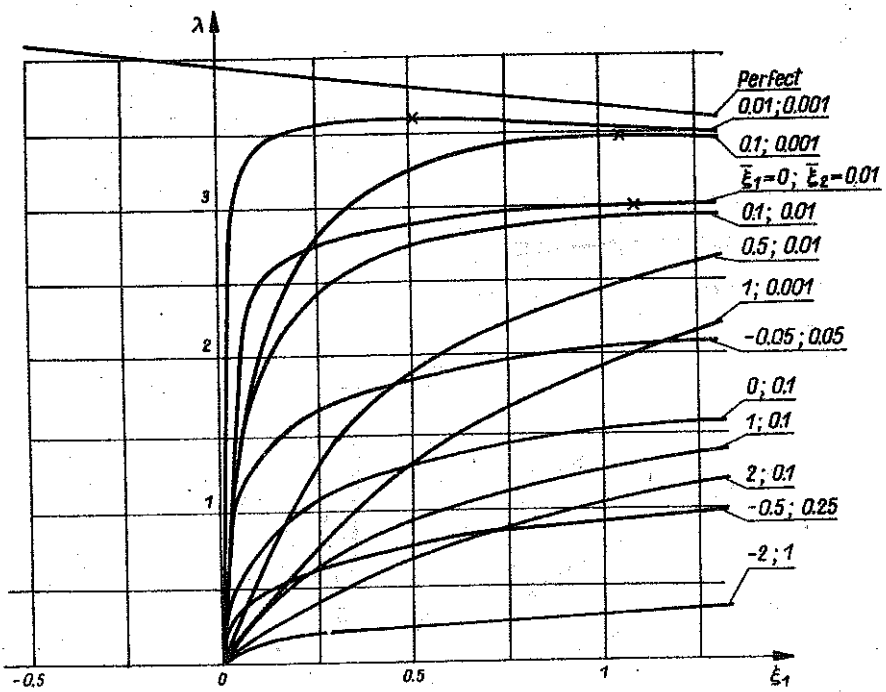

FIG. 5. Load versus overall mode displacement ξ_1 for wide plate $b_2/b_1 = 0.7166$, $b_3/b_1 = 0.4933$, $b_4/b_1 = 1.0$, $l/b_1 = 12$, $h_2/h_1 = 0.6$, $h_3/h_1 = 0.6$, $b_1/h_1 = 30$, $m = 20$.

In the other cases the maximum carrying capacity is not reached in the considered range. The influence of the overall buckling mode is defined by the generalized displacement parameter $z_1 = -d_3 \xi_1$ ($z_1 = 1 - \lambda/\lambda_2$) of which the positive growth of z_1 accompanies the growth of the imperfection-sensitivity. In the cases shown in Figs. 3 and 4 the post-buckling coefficients d_2 and d_3 are greater than zero ($d_2 > 0, d_3 > 0$) and in Fig. 5 the coefficients are less than zero ($d_2 < 0, d_3 < 0$).

Figures 3 and 4 show the strong sensitivity to the negative overall mode imperfections $\bar{\xi}_1$ explained by the asymmetric post-bifurcation behaviour $z_1 \geqslant 0$ and the sensitivity to positive imperfections $\bar{\xi}_1$ mainly due to the interaction with the local mode.

Figure 5 shows the strong sensitivity to positive imperfections $\bar{\xi}_1$ and the sensitivity to negative $\bar{\xi}_1$.

The post-bifurcation behaviour of the wide plate with imperfections $\bar{\xi}_1 = 0.05$, $\bar{\xi}_2 = 0.05$; $\bar{\xi}_1 = 0.5$, $\bar{\xi}_2 = 0.25$ and $\bar{\xi}_1 = 2.0$, $\bar{\xi}_2 = 1.0$ is shown in Figs 3 and 4.

The bifurcation mode amplitude $\bar{\xi}_1$ initially grows in the direction of ξ_1 (positive ξ_1) but finally is forced by the local imperfections to change the sign in the direction of positive z_1 ($\xi_1 < 0$) just before the maximum load is reached. The same effect is seen from the curves for $\bar{\xi}_1 = -0.05$, $\bar{\xi}_2 = 0.05$; $\bar{\xi}_1 = -0.5$, $\bar{\xi}_2 = 0.25$ and $\bar{\xi}_1 = -2.0$, $\bar{\xi}_2 = 1.0$ in Figs. 5 as it has been already mentioned above (initially grows in the negative ξ_1 and finally changes in the positive ξ_1 ($z_1 > 0$)). Initial imperfections lower the maximum carrying capacity in all the considered cases.

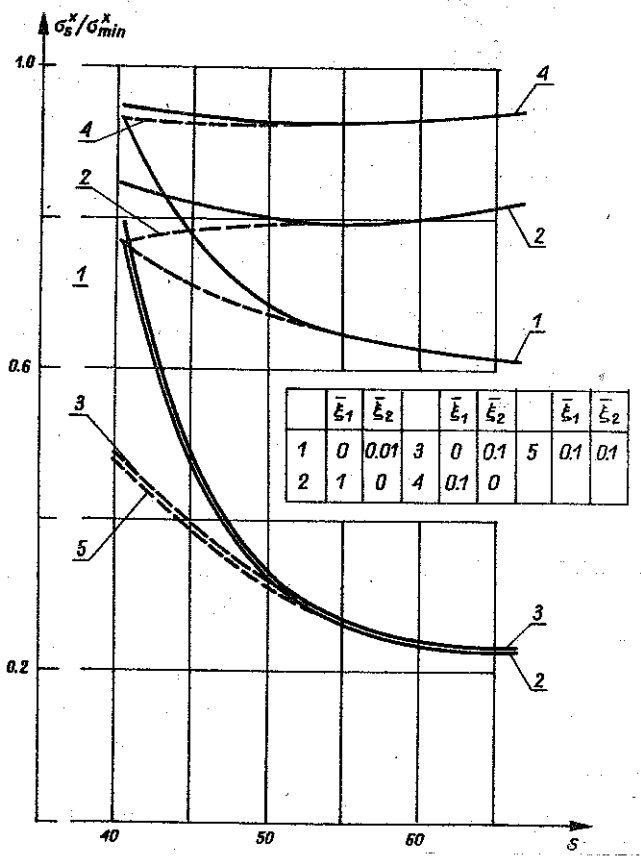

FIG. 6. Relationship between $\sigma_s^*/\sigma_{min}^*$ and eigenvalent slenderness ratio s for several values of $\bar{\xi}_1$ and $\bar{\xi}_2$

$b_4/b_1 = 1$, $h_2/h_1 = h_3/h_1 = 0.6$, $b_1/h_1 = 30$, $\alpha = \arccos\left(\frac{b_1 - b_2}{2b_2}\right) \approx 70°$.

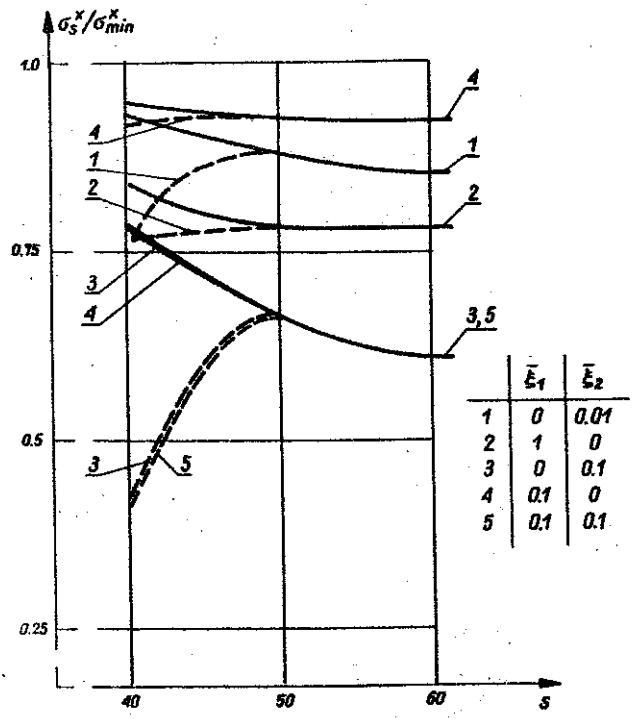

FIG. 7. Relationship between $\sigma_s^*/\sigma_{\min}^*$ and s for several values of $\bar{\xi}_1$ and $\bar{\xi}_2$
$b_2/b_1 = 0.7166$, $b_3/b_1 = 0.4933$, $h_2/h_1 = h_3/h_1 = 0.6$, $b_1/h_1 = 30$.

Figures 6 and 7 show graphs of the ratio $\sigma_s^*/\sigma_{\min}^*$ (where $\sigma_{\min}^* = \min(\sigma_1^*, \sigma_2^*)$) as a function of the equivalent slenderness s of the $ABCD$ segment (Fig. 2) at different imperfection amplitudes $\bar{\xi}_1$ and $\bar{\xi}_2$, referred to the skin-plate thickness h_1. The impefection amplitude $\bar{\xi}_1$ has been selected so that the value of $\bar{z}_1$ should not be less than zero ($\bar{z}_1 = -\bar{\xi}_1, d_3 \geqslant 0$) because in this case the interaction of the local and global buckling modes will result in a decrease of limit stress σ_s^*. In Figs. 6 and 7 full lines show the results obtained for the first local buckling mode corresponding to σ_2^*, the number of half-waves being $m = 13$, while the broken lines refer to the results of the other local mode, which corresponds to σ_3^* at $m = 20$. Then the interaction of the global mode with each of the local modes separately has been considered. In this way a nondimensional limit stress σ_s^* has been obtained as a function of the number of half-waves m for the different imperfection amplitudes $\bar{\xi}_1$ and $\bar{\xi}_2$, which is shown in Fig. 8. Furthermore, in each case a set of three nonlinear equations (4.4) have been solved for two local modes at different half-waves number m and for the global buckling mode with the application of the condition that the Jacobian of this set of equations must be zero. Numerical calculations have proved that the interaction of local modes is very weak or absent.

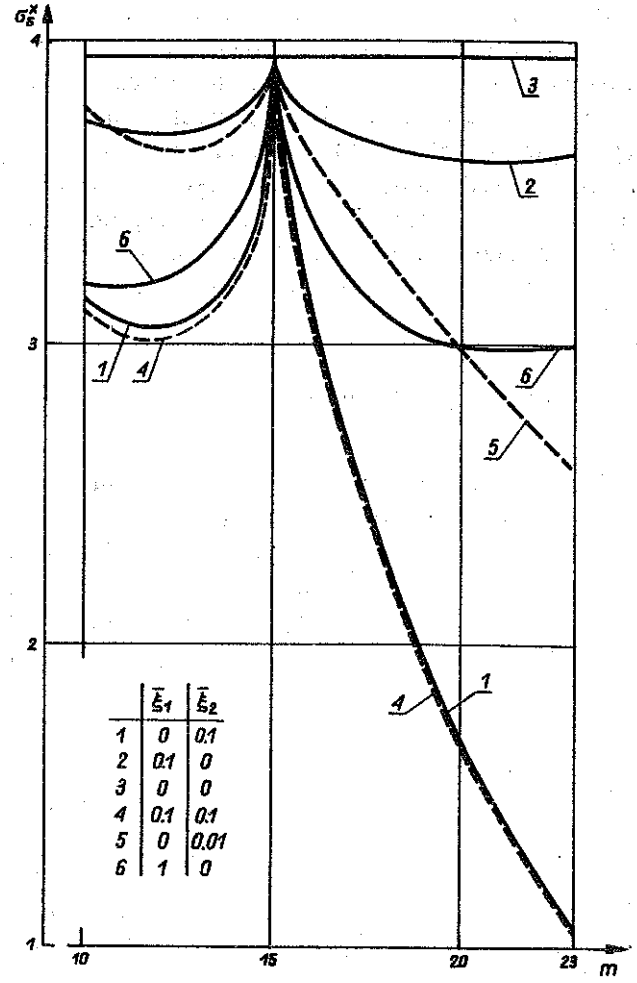

FIG. 8. Relationship between limit dimensionless stress σ_s^* and number of half-waves m for plate's geometry
$b_2/b_1 = 0.7166$, $b_3/b_1 = 0.4933$, $b_4/b_1 = 1.0$, $l/b_1 = 12$, $h_2/h_1 = h_3/h_1 = 0.6$, $b_1/h_1 = 30$.

For the number of half-waves $m \leqslant 15$ the obtained coefficients d_2 and d_3 have been positive, and for $m \geqslant 16$ negative, which causes a significant increase in the sensitivity to imperfections. The coefficients d_2 and d_3 of the system (4.4) are the sums of integrals of different signs and they depend on the ratios of displacement amplitudes of particular plates. The selection of the imperfection amplitude has been similar to the previous one, i.e. it has been done so that $\bar{z}_1 \geqslant 0$. Moreover, a comparison has been made between the obtained results from Table 1 and the results obtained on the base of TVERGAARD'S work [5].

However, even in the linear analysis the significant differences have been found when beam- and plate-models of stiffeners were assumed.

It can easily be noticed that the maximum value of $|d_3|$ and minimum of σ_2^* is in the general case achieved at different values of m. The complex nature of dependence of σ_s^* on the number of half-waves m causes that the most dangerous local modes in linear and nonlinear analysis may be different. The conclusions reported here are convergent with those obtained by MANEVIČ [14, 15 and 16] for cylindrical shells and plate strengthened with stiffeners of the rectangular and T-bar section.

6. CONCLUSIONS

The initial post-buckling behaviour of the infinitely wide plate with thin-walled longitudinal stiffeners of trapezoidal cross-section has been determined. The solutions given here are valid in cases of uniform compression. In the case when a few buckling modes are comparable, disregarding mode interaction may lead to overestimating the useful load capacity. On the ground of nonlinear analysis, reduction of the imperfection-sensitivity of the plate can be reached by a selection of the geometric parameters.

APPENDIX. THE ASYMPTOTIC METHOD

The method outlined in the following was developed by BYSKOV and HUTCHINSON in [1] where a complete derivation is given. This method is suitable for structures with M simultaneous or nearly simultaneous buckling modes.

Assume that the structure is perfect and that the prebuckling state is linear with respect to the scalar load parameter λ. The displacement field is expanded in the following fashion:

$$u = \lambda u_0 + \xi_i u_i + \xi_i \xi_j u_{ij} + \dots, \tag{A.1}$$

where the prebuckling displacement field is described by λu_0, the amplitude ξ_i measures the influence of the buckling mode u_i, and u_{ij} is the second order field associated with u_i and u_j. Summation from 1 to M is implied for repeated Latin lower-case indices.

The stress and strain fields are expanded in a fashion similar to (A.1)

$$\begin{aligned} \sigma &= \lambda \sigma_0 + \xi_i \sigma_i + \xi_i \xi_j \sigma_{ij} + \dots, \\ \varepsilon &= \lambda \varepsilon_0 + \xi_i \varepsilon_i + \xi_i \xi_j \varepsilon_{ij} + \dots. \end{aligned} \tag{A.2}$$

The strain-displacement relation can be written in the form

(A.3) $$\varepsilon = l_1(u) + 1/2\, l_2(u),$$

where l_1 and l_2 are linear and quadratic operators, respectively. A bilinear operator l_{11} is defined by

(A.4) $$l_2(u+v) = l_2(u) + 2l_{11}(u, v) + l_2(v).$$

The linear of the prebuckling state is characterized by

(A.5) $$l_{11}(u_0, v) = 0$$

for any v which in turn implies

(A.6) $$\varepsilon_0 = l_1(u_0).$$

The material is assumed to be linearly elastic so that the stress σ is given by

(A.7) $$\sigma = H(\varepsilon),$$

where H designates a linear operator.

The dot notation used in the folloving denotes integration over the entire structure

(A.8) $$\sigma \cdot \varepsilon = \int_v \sigma_{ij}\, \varepsilon_{ij} \cdot dV.$$

The eigenvalue problems determining the buckling modes and their associated eigenvalues λ_J are found the variational equation

(A.9) $$\sigma_J \cdot l_1(\delta u) + \lambda_J\, \sigma_0 \cdot l_{11}(u_J, \delta u) = 0, \quad J = 1, \ldots, M,$$

where δu denotes all kinematically admissible variations of u. The buckling modes are taken to be mutually orthogonal in the following sense:

(A.10) $$\sigma_0 \cdot l_{11}(u_i, u_j) = 0, \quad i \neq j.$$

The second order and all possible higher order fields may be shown to be orthogonal to all buckling modes in the sense of Eq. (A.10). For a displacement field u the amplitude ξ_J of its component in the shape of u_J is defined by

(A.11) $$\sigma_0 \cdot l_{11}(u, u_J) = \xi_J\, \sigma_0\, l_2(u_J).$$

A variational statement of the second order boundary value problem is

(A.12) $$\sigma_{ij} \cdot l_1(\delta u) + \lambda \sigma_0 \cdot l_{11}(u_{ij}, \sigma u) = -1/2\,(\sigma_i \cdot l_{11}(u_j, \delta u) + \sigma_j \cdot l_{11}(u_i, \delta u)),$$

where u_{ij} and δu are orthogonal to each u_k in the sense of Eq. (A.10), and $\lambda = \lambda_c = \min(\lambda_J)$.

The right hand side of this expression is symmetric in the indices. If the structure suffers geometric imperfections $\bar{u}$ given by

$$\bar{u} = \bar{\xi}_i u_i, \tag{A.13}$$

the following M nonlinear equations determine the equilibrium paths

$$\xi_J \left(1 - \frac{\lambda}{\lambda_J}\right) + \xi_i \xi_j a_{ijJ} + \xi_i \xi_j \xi_k b_{ijkJ} = \frac{\lambda}{\lambda_J} \bar{\xi}_J, \quad J = 1, \ldots, M. \tag{A.14}$$

The formulas for the coefficients are

$$a_{ijJ} = [\sigma_J \cdot l_{11}(u_i, u_j) + 2\sigma_i \cdot l_{11}(u_j, u_J)]/(2\sigma_j \varepsilon_J)$$

and

$$b_{ijkJ} = [\sigma_{Ji} \cdot l_{11}(u_j, u_k) + \sigma_{ij} \cdot l_{11}(u_k, u_J) + \sigma_J \cdot l_{11}(u_i, u_{jk}) + \\ + \sigma_i \cdot l_{11}(u_J, u_{jk}) + 2\sigma_i \cdot l_{11}(u_j, u_{kJ})]/(2\sigma_j \varepsilon_J). \tag{A.15}$$

REFERENCES

1. E. BYSKOV and J. W. HUTCHINSON, *Mode interaction in axially st ffened cylindrical shells*, AIAA J., **15**, 7, 1977.
2. J. W. HUTCHINSON and J. C. AMAZIGO, *Imperfection-sensitivity of eccentrically stiffened cylindrical shells*, AIAA J., **5**, 3, 1967.
3. W. T. KOITER and M. PIGNATARO, *An alternative approach to the interaction between local and overall buckling in stiffened panels*, Buckling of Structures, Proc. IUTAM Symposium, 1976.
4. W. T. KOITER, *General theory of mode interaction in stiffened plate and shell structures*, WTHD, Report 590, Delft, Holland 1976.
5. V. TVERGAARD, *Imperfection-sensitivity of a wide integrally stiffened panel under compression*, Inter. J. Solids and Struct., **9**, 1, 1973.
6. V. TVERGAARD, *Influence of post-buckling behaviour on optimum design of stiffened panels*, Inter. J. Solids and Struct., 9, 2, 1973.
7. A. VAN DER NEUT, *Mode interaction with stiffened panels*, Buckling of Struct., Proc. of IUTAM Symposium, 1976.
8. F. W. WILLIAMS, W. H. WITTRICK and R. J. PLANK, *Critical buckling loads of some prismatic plate assemblies*, Buckling of Struct Proc. of IUTAM, Symposium, 1976.
9. W. C. FOK, J. RHODES and A. C. WALKER, *Local buckling of outstands in stiffened plates*, Aeronaut. Quart., 127, 1976.
10. W. C. FOK, A. C. WALKER and J. RHODES, *Buckling of locally imperfect stiffeners in plate*, J. Eng. Mech. Div., Proc. Amer. Soc. Civ. Eng., **103**, 5, 1977.
11. А. И. МЕНЕВИЧ, *Взаимодействие форм потери устойчивости сжатой подкрепленной панели*, Строит. мех. и расчет сооруж., 5, 1981.
12. G. SEDLACEK, *Einzelfeldbeulnachweise für rippenversteifte Blache*, Techn. Mitt. Krupp–Forsch–Ber, **35**, 2, 1977.
13. T. SHIGEMATSU, T. HARA and M. OHGA, *Untersuchung der Stabilität einseitung gedrücker ländgsansgesteifter ortotroper Rechteckplatten mit Schubverformung*, Der Stahlbau, 6, 1982.
14. А. Й. МАНЕВИЧ, *К теории связанной потери устойчивости подкрепленных тонкостенных конструкций*, Прикладная матем. и механ., **46**, 2, 1982.

15. А. Й. Меневич, *Потеря устойчивости сжатых продольно подкрепленных цилиндрических оболочек при конечных перемещениях с учетом локального выпучивания ребер-пластин*, Механика твердого тела, 2, 1983.
16. А. Й. Маневич, *Устоичивость пластин и оболочек с ребрами*, Строит, мех. и расчет сооруж., 3, 1984.
17. E. Byskov and J. C. Hansen, *Postbuckling and imperfection sensitivity of axially-stiffened cylindrical shells with mode interaction*, DCAMM, 163, 1979.
18. J. Singer and R. T. Hafka, *Buckling of discretely stringer-stiffened cylindrical shells and elastically restrained panels*, AIAA J., **13**, 7, 1975.
19. S. P. Chang, *Beitrag zur Berechungung des nichlinearen Traverhaltens einer in Langsrichtung mit offenen oder geschlossenen Steifen verstarkten und durch Druck belasteten Rechteckplatte mit Vorverformungen bei Navierschen Randbedingungen*, Dissertation, Universität Stuttgart, 1976.
20. H. J. Langhoff and M. Granzen, *Fabrication of box gurder bridges, Steel box girder bridges*, W. Clowers and Sons. Ltd, London 1973.
21. W. T. Koiter, *Current trends in the theory of buckling*, Buckling of Struct., Proc. IUTAM Symposium, 1976.

Streszczenie

WZAJEMNE ODDZIAŁYWANIE POSTACI WYBOCZENIA SZEROKIEJ PŁYTY WZMOCNIONEJ WZDŁUŻNYMI ŻEBRAMI ZAMKNIĘTYMI, PODDANEJ ŚCISKANIU

W pracy przeanalizowano wyboczenie ściskanej nieskończenie szerokiej płyty wzmocnionej wzdłużnymi żebrami zamkniętymi przy uwzględnieniu wzajemnego oddziaływania prawie równoczesnych postaci wyboczenia. Żebra modeluje się płytami. Uwzględniono wpływ niedokładności na wartość obciążenia granicznego. Zagadnienie rozwiązano na podstawie asymptotycznej teorii pobifurkacyjnego wyboczenia konstrukcji sprężystych.

Резюме

ВЗАИМНОЕ ВОЗДЕЙСТВИЕ ВИДОВ ПРОДОЛЬНОГО ИЗГИБА ШИРОКОЙ ПЛИТЫ, УПРОЧНЕННОЙ ПРОДОЛЬНЫМИ ЗАМКНУТЫМИ РЕБРАМИ, ПОДВЕРГНУТОЙ СЖАТИЮ

В работе проанализирован продольной изгиб сжимаемой бесконечно широкой плиты, упрочненной продольными замкнутыми ребрами, при учете взаимного воздействия почти одновременных видов продольного изгиба. Ребра моделируются плитами. Учтено влияние неточности на значение предельной нагрузки. Задача решена, опираясь на асимптотическую теорию послебифуркационного продольного изгиба упругих конструкций.

TECHNICAL UNIWERSITY OF ŁÓDŹ, ŁÓDŹ.

Received July 11, 1986.